Available online at www.sciencedirect.com
SCIENCE DIRECT
Surface & Coatings Technology 197 (2005) 1–9
SURFACE & COATINGS TECHNOLOGY
www.elsevier.com/locate/surfcoat

Friction and wear behavior of vacuum plasma-sprayed Ti–Zr–Ni quasicrystal coatings

P.P. Bandyopadhyay[a], S. Siegmann[b,*]

[a]Bengal Engineering and Science University, Howrah, India
[b]EMPA-Materials Science and Technology, Thun-3602, Switzerland

Received 6 January 2004; accepted in revised form 5 November 2004
Available online 6 April 2005

Abstract

This investigation deals with a study of the friction and wear behavior of vacuum plasma sprayed quasicrystal (QC) $Ti_{41.5}Zr_{41.5}Ni_{17}$ coatings. During ball on disc experiments, a change in the mode of wear has been found to occur with corresponding changes in ball material, normal load and sliding velocity. The low thermal conductivity of quasicrystals and its brittleness play a vital role in determining the friction and wear behavior of such materials. When these coatings are subjected to rubbing for a longer period of time, wear occurs by subsurface crack propagation and subsequent delamination within the coated layer.

Keywords: Quasicrystal; Plasma spraying; Pin on disc; Scanning electron microscopy

1. Introduction

The discovery of quasicrystal (QC) [1] phases has been reported in 1984. Such phases offer outstanding material properties, e.g., high hardness [2,3], low friction coefficient [4], low surface energy [5], high thermo-electric power [6], etc. Thus quasicrystals are potential candidates for many industrial applications [7–9].

To date, quite a few alloys containing a quasicrystal phase have been identified [10]. Some of them are stable and worthy of investigations concerning their application potential in the engineering domain. The i-phase of $Ti_{41.5}Zr_{41.5}Ni_{17}$ constitutes one such system [11]. This phase reportedly is capable of storing hydrogen in large quantities [12] and hence is a highly potential candidate for fuel cell application. The i-phase develops in the prior Laves and alpha phase (both HCP) eutectic matrix upon annealing at 570 °C for 7 days [13]. Further annealing at a lower temperature does not cause any transformation of the i-phase. It indicates that the QC phase in question is very stable [11].

Quasicrystals in general are not produced by conventional fabrication techniques. They cannot be formed or cast readily. As stated, the growth of the i-phase in the $Ti_{41.5}Zr_{41.5}Ni_{17}$ alloy also involves prolonged annealing of the cast ingots. However, alloys having the composition of a QC can be reduced to powder and subsequently can be thermally sprayed to form a thick coating having the QC phase [14–18]. This phenomenon can be attributed to the rapid quenching associated with the thermal spraying processes.

To date, a few reports are available highlighting the tribological aspects of quasicrystal coatings [7,8,10,17,19]. In general, these studies are limited to Aluminium based quasicrystals. While these materials are expected to yield a high wear resistance and a low coefficient of friction they apparently are somewhat limited by their brittleness [7]. To combat such brittleness, composite quasicrystal coatings incorporating a ductile phase as a matrix material have been developed on an experimental basis [19]. The study of friction and wear of quasicrystals are still very much under development.

This paper, to the knowledge of the authors, is the first report on the tribological aspects of $Ti_{41.5}Zr_{41.5}Ni_{17}$ quasicrystal coating. The other pertinent feature of such coatings,

* Corresponding author. Tel.: +41 33 228 2945; fax: +41 33 228 4490.
E-mail address: stephan.siegmann@empa.ch (S. Siegmann).

0257-8972/$ - see front matter © 2004 Published by Elsevier B.V.
doi:10.1016/j.surfcoat.2004.11.009

e.g., phases, microstructure and coating integrity, has been presented in another report [20].

2. Experimental

$Ti_{41.5}Zr_{41.5}Ni_{17}$ powder with a size fraction of −70+10 μm has been prepared by gas atomization of the alloy in argon environment. This powder has been vacuum plasma sprayed on stainless steels substrates using a Medicoat 50 kW plasma spraying facility equipped with a six-axes robot. Before spraying, the substrates have been grit blasted with alumina grits to a surface roughness of Ra=5 μm. Prior to the final spraying, a set of trial runs have been made using various parameter sets and the process was monitored online using a DPV 2000 particle diagnostic system. This instrument is capable of monitoring the particle velocity and temperature online during spraying and hence enables the user to ensure that the particle temperature is above the melting temperature and it has acquired an adequately high velocity to effect plastic deformation during the impact with the substrate. These conditions must be fulfilled to effect proper splat formation. The parameters used to prepare the final set of coatings are listed in Table 1. Substrates made of 304 stainless steel with a diameter of 40 mm and thickness 6 mm have been used in these experiments.

The structural analysis of the powders and coatings has been carried out using a Siemens D 5000 X-ray diffractometer with MoK_α radiation. The XRD data thus obtained has been represented as its CuK_α equivalent in this paper for comparison purpose [21]. The polished and etched cross sections have been subsequently examined under an optical microscope. The porosity of the coatings has been measured by image analysis using the Zeiss KS 400 software. The Vickers hardness of the coatings has been measured using a Leitz Wetzlar hardness tester under a load of 100 g. An average of 10 readings has been reported. The adhesion strength of the coatings has been measured in accordance with the standard EN 582.

The friction and wear measurements have been conducted at room temperature, using a CSEM Pin-on-Disc tribometer, which permits rotation of a flat specimen against a stationary pin or ball. During the tests, the coefficient of friction (COF) has been monitored continuously. Prior to the tests, the disc samples have been polished to a surface roughness of Ra=0.2 μm. Every trial has been conducted on a fresh track and the specimen has been cleaned ultrasonically in alcohol immediately before the test. The measurement of coefficient of friction has been done with two different ball materials, namely ZrO_2 and 100Cr6 steel. For wear measurement only the ZrO_2 ball has been used. The ball diameter is 10 mm. The reported mass loss in wear reflects an average of three readings. The parameters for the ball on disc tests are listed in Table 2. Both the surfaces and polished cross sections of the worn specimens have been observed under a Zeiss DSM 962 Scanning Electron Microscope (SEM) equipped with EDS facility. The thermal diffusivities of the coatings (both in-plane and through thickness) have been measured by the laser flash method and the corresponding thermal conductivities have been calculated from the measured data.

Table 1
Parameters for vacuum plasma spraying

Parameters	Units	Values
Chamber pressure	mbar	120
Standoff distance	mm	400
Primary gas (Ar) flow rate	sl/min	50
Secondary gas (He) flow rate	sl/min	10
Arc current	amp	700
Nozzle diameter	mm	6
Powder carrier gas flow rate	sl/min	1.3

Table 2
Parameters for ball on disc tests

Purpose	Ball material	Normal load (N)	Sliding velocity (m/s)	Sliding distance (m)
Measurement of COF	ZrO_2	5, 10, 20, 25 and 30	0.1, 0.2, 0.4, 0.6. 0.8 and 1.0	10
	100Cr6 steel	5, 10, 20 and 30	0.1, 0.2, 0.4, 0.6. 0.8 and 1.0	10
Measurement of mass loss owing to wear	ZrO_2	10	0.5	10, 20, 50, 100, 200, 500 and 1000

3. Results and discussion

3.1. Coating microstructure and phases

This aspect has been treated in detail in another paper [20]. In this paper, a few important features are discussed briefly.

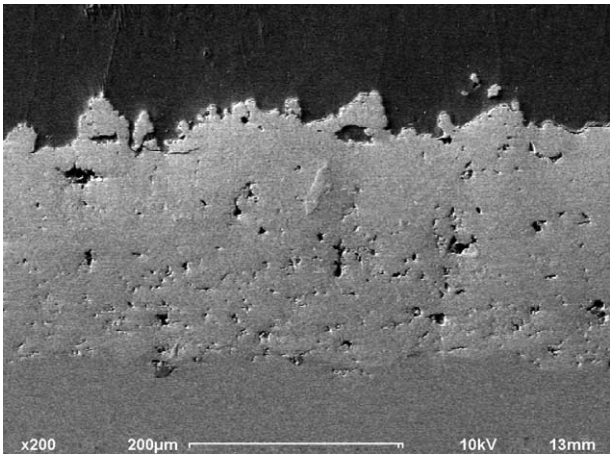

Fig. 1. SEM micrograph of the as-polished cross-sections of the coating produced from the $Ti_{41.5}Zr_{41.5}Ni_{17}$ powder.

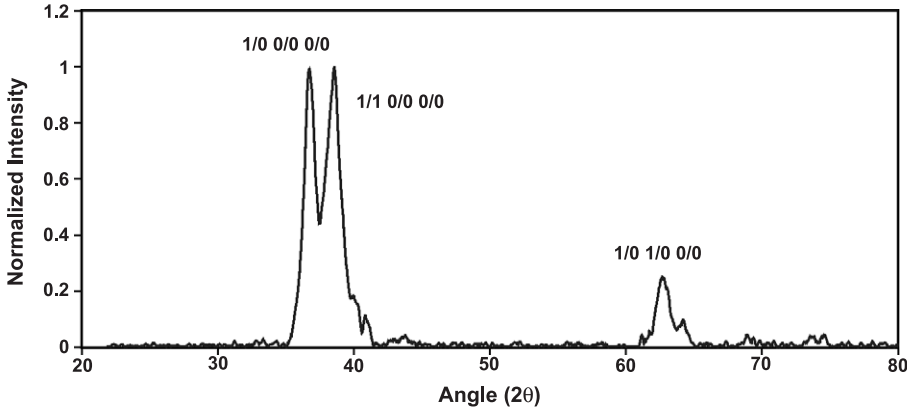

Fig. 2. Diffractogram of the as-sprayed coating (corrected for CuK_{α} radiation).

Fig. 1 shows the SEM micrograph of the as-polished cross sections of the coating produced from the $Ti_{41.5}Zr_{41.5}Ni_{17}$ powder. The coating has a splat morphology with scattered pores, characteristic of thermally sprayed coatings. The individual particles are well molten and the coating is well adherent to the substrate (bond strength 73.5 MPa). The coating porosity is found to be 4.9 vol.% and the hardness recorded is $631.5HV_{0.1}$. Limited porosity, presence of very few unmelted particles and good adherence of the coating with the substrate speaks of good coating integrity. Fig. 2 shows the diffractogram of the as-sprayed coating. The two major peaks present belong to the quasicrystal phase and it indicates the coating contains a significant amount of the QC i-phase [21]. In addition, an EDS study of the microstructure indicates the presence of Laves phase as well [20].

3.2. Coefficient of friction

The nature of variation of the coefficient of friction under different sliding velocities and normal loads against zirconia and steel balls are plotted in Figs. 3 and 4, respectively. In both cases, the coefficient of friction is found to decrease with increase in either sliding velocity or load. In general, this trend is more prominent in case of the zirconia ball. Fig. 5 is a low magnification secondary electron (SE) image of the coated surface bearing three wear tracks created by zirconia balls sliding at a velocity of 0.5 m/s and normal loads of 25 N (uppermost track), 10 N (middle track) and 5 N (lowermost track), respectively. From this image, it is evident that a higher load brings about considerably higher plastic deformation on the surface.

Fig. 6a–c corresponds to the wear track for a load of 5 N and a sliding velocity of 0.5 m/s. The wear track consists of parallel (Fig. 6a) lines, caused apparently by abrasion and indicative of limited plastic deformation. Fig. 6b shows the presence of a few fractured particles on the wear track. An EDS analysis of the particles reveals that these particles are broken out fragments of the zirconia rubbing ball. Fig. 6c shows the unsteady nature of the coefficient of friction during sliding. It is speculated that at a lower load the temperature of the contact is low enough for the NZT coating to retain its hardness. Rubbing between two hard objects results in a limited amount of plastic deformation of the coating and the fracture of the zirconia ball. The sharp edges of the partly broken zirconia ball causes abrasion of the coating. The unsteady friction coefficient is a result of

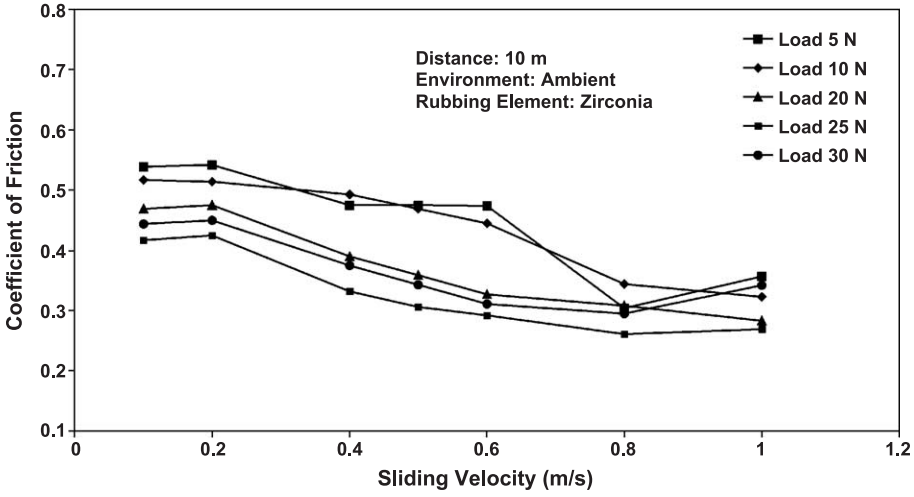

Fig. 3. Variation of coefficient of friction of Ti–Zr–Ni coating during rubbing against zirconia ball at different normal loads and sliding velocities.

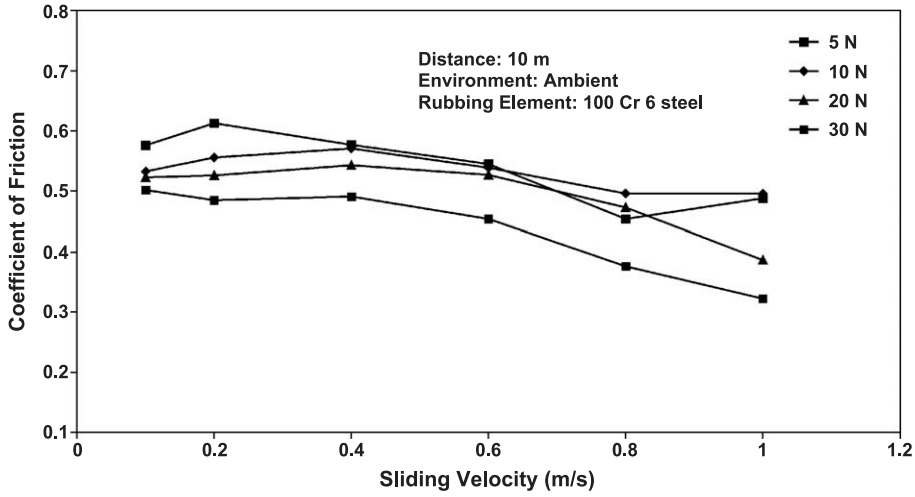

Fig. 4. Variation of coefficient of friction of Ti–Zr–Ni coating during rubbing against 100Cr6 steel ball at different normal loads and sliding velocities.

both the vibration of the instrument in the vertical direction under a low load and a stick-slip phenomenon at the contact region. Fig. 7a–c corresponds to the wear track for a load of 10 N and describe a scenario very similar to that of Fig. 6. Contact between the two hard surfaces causes fracture of the zirconia ball. The broken off particles are shown in Figs. 6b and 7b. Once again, the sharp edges of the partially broken zirconia ball abrade on the coating surface. The increase in load, however, restricts both the instrument vibration and stick-slip, thus limiting the rapid changes in the coefficient of friction with sliding distance (Figs. 6c and 7c).

Figs. 8 deal with the nature of friction and wear at a normal load of 30 N. Fig. 8a and b shows that, in contrast to the lower load scenario, considerable plastic deformation and side flow occurs when the normal load is increased to 30 N. The coefficient of friction (Fig. 8c) shows a steady decrease during sliding. There is no fractured zirconia particle present on the wear track. Possibly, at this load, the temperature of the contact region is high enough to soften the coating. The calculated thermal conductivities of the coating obtained from the measured thermal diffusivities are 3.15±0.1 W/mK (through thickness) and 2.06±0.08 W/mK (in-plane). The thermal conductivity of sintered zirconia ceramic is around 1.8 W/mK. So the thermal conductivity of this coating is comparable to that of zirconia. Low heat conductivities of the quasicrystal and zirconia aid the heat retention process [8,22]. The softened coating yields quickly under the rubbing zirconia ball and provide a low friction path to the motion. So the mean coefficient of friction is found to be low at this load.

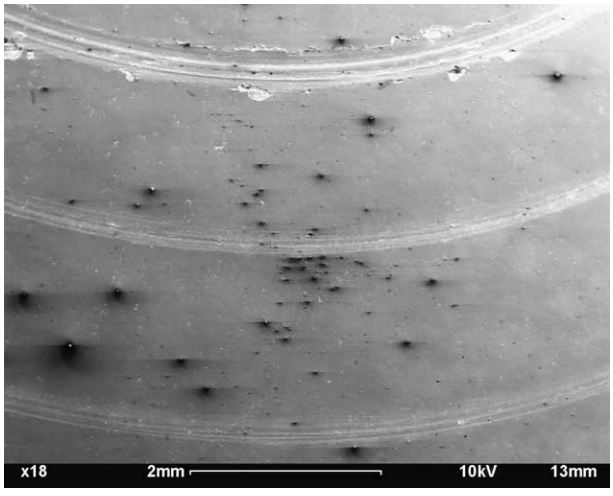

Fig. 5. The SE image of the QC coating bearing three wear tracks created by zirconia balls sliding at a constant sliding velocity of 0.5 m/s and normal loads of 25 N (uppermost track), 10 N (middle track) and 5 N (lowermost track), respectively.

Fig. 9 is an overview of the effect of variation in sliding velocity on the mechanism of wear and friction of the coating in question, at a constant load. It is a low magnification SE image of the wear tracks left on the disc by zirconia balls travelling at 0.1 m/s (top), 0.2 m/s (middle) and 0.4 m/s (bottom), respectively, while transmitting a constant normal load of 25 N on the coating surface. The first two have left an array of parallel clear rubbing marks, suggestive of abrasion. The third, i.e., the one corresponding to a velocity of 0.4 m/s, reflects considerable plastic deformation and side flow.

Fig. 10a corresponds to a sliding velocity of 0.1 m/s. It is speculated that, in such a low velocity regime, the temperature of the contact region is low and the coating can retain its hardness. The zirconia ball undergoes fracture and the sharp edges of the fractured zirconia ball causes abrasion on the coating surface. Fig. 10a shows the presence of a large number of fractured zirconia particles. Fig. 10b is a record of the variation of the coefficient of friction with sliding distance. Its saw tooth nature and the high mean value of the coefficient of friction is suggestive of a stick-slip nature of motion. An increase in the sliding velocity to 0.4 m/s causes a major change in the mode of friction between the rubbing pair. Fig. 11a shows the presence of a plastically deformed continuous layer on the surface. No fractured zirconia particle is detected on the surface. The coefficient of friction

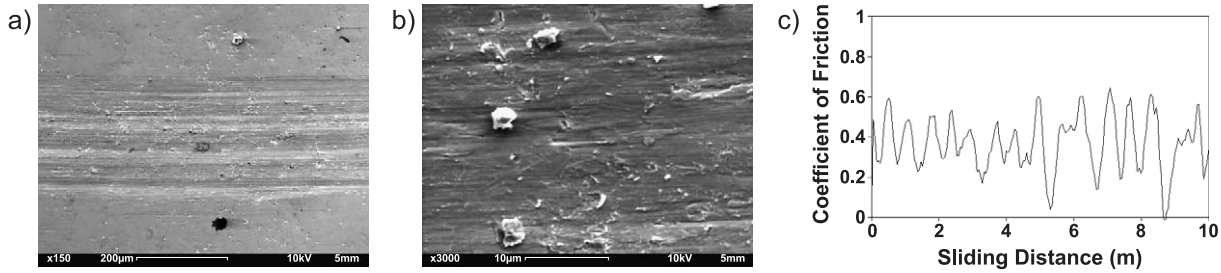

Fig. 6. (a) SE images and (b) higher magnifications of the wear tracks on the QC coating caused by a zirconia ball including (c) the corresponding coefficients of friction for 5 N at a sliding velocity of 0.5 m/s.

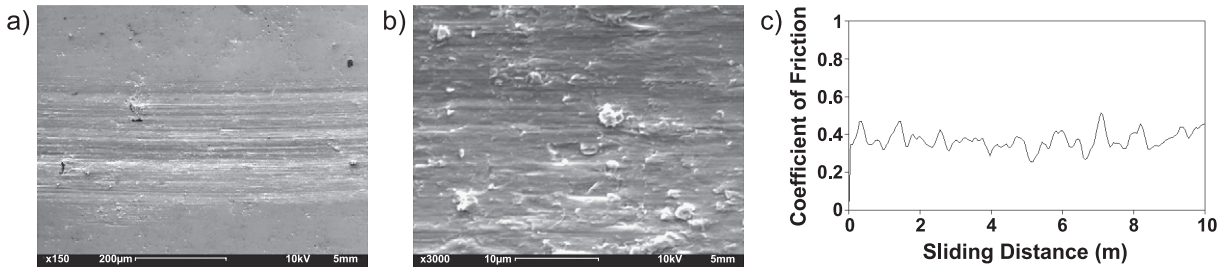

Fig. 7. (a) SE images and (b) higher magnifications of the wear tracks on the QC coating caused by a zirconia ball including (c) the corresponding coefficients of friction for 10 N at a sliding velocity of 0.5 m/s.

plot (Fig. 11b) shows minor variation with sliding distance. The magnitude of the coefficient of friction obtained is also less than the same at a sliding velocity of 0.1 m/s. Once again, an increase in sliding velocity brings about an effect similar to the one obtained by an increase in the normal load. At high sliding velocity, the frictional heat generation at the contact is likely to be high and this results in softening of the coating immediately below the zirconia ball. The low thermal conductivity of both the rubbing elements helps heat retention and severe plastic deformation of the softened coating takes place.

The above experiment has been repeated with a 10-mm diameter 100Cr6 steel ball. Figs. 12a and 13a show higher magnification of wear tracks created by steel balls acting on the coating surface with a normal load of 10 N (Fig. 12) and 30 N (Fig. 13), respectively. The sliding velocity in both cases is 0.5 m/s. The nature of wear presumably is abrasive in both cases. In addition, the extent of surface damage in both cases are comparable in spite of the difference is normal load. In this case, the plastic deformation of the surface is not significant and the mode of interaction between the rubbing pair is abrasive. The coefficient of friction shows some variation with respect to sliding distance, which can be attributed to vibration at low load. An increase in normal load does not bring about any major changes in the wear mode in the case of steel ball. This can be attributed to a higher thermal conductivity of steel as compared to zirconia. Higher load causes generation of a higher amount of heat, which is conducted away through the steel ball. The bulk temperature of the contact area appears to remain relatively stable and the coating retains its hardness to a great extent. However, Fig. 13b shows a slow but steady decrease in coefficient of friction after first 2 m of sliding. Possibly, this is indicative of limited softening and plastic deformation at the contact region and the resulting decrease in the average coefficient of friction with load. Fig. 14a and b shows the effect of increase in sliding velocity from 0.1 to 0.8 m/s at a constant load of 30 N using a steel ball as rubbing element. It appears that the mechanism of wear in both cases is abrasive and an increase in sliding velocity does not bring about a significant change in such mechanism. However, the reduction in coefficient of friction

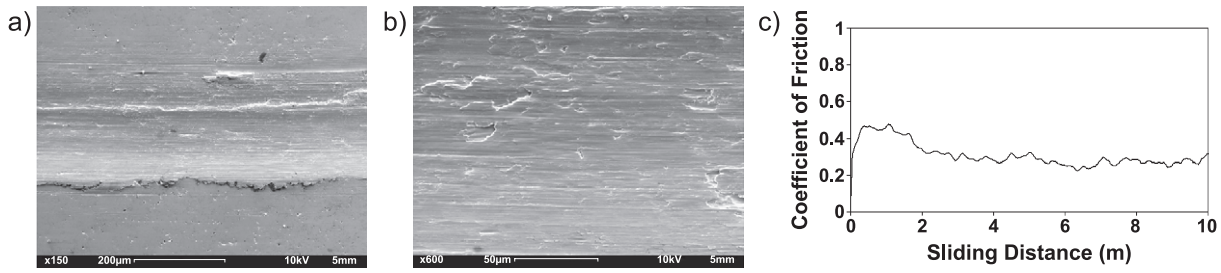

Fig. 8. (a) SE images and (b) higher magnifications of the wear tracks on the QC coating caused by a zirconia ball including (c) the corresponding coefficients of friction for 30 N at a sliding velocity of 0.5 m/s.

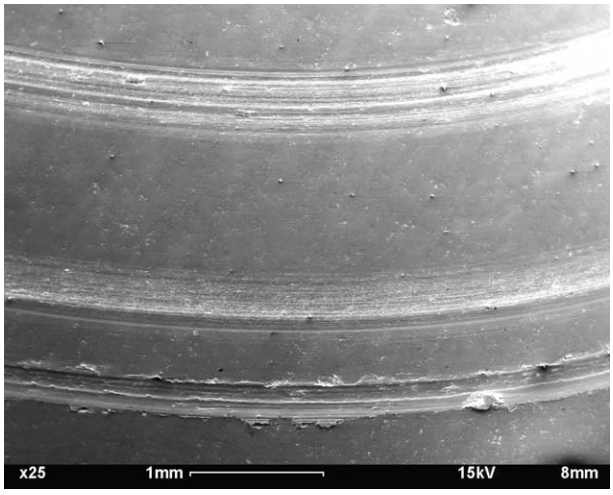

Fig. 9. The SE image of the coating showing three wear tracks created by zirconia balls rubbing on the QC coating surface as a function of the sliding velocity: 0.1 m/s (top), 0.2 m/s (middle) and 0.4 m/s (bottom). The normal load was 25 N in all cases.

under this circumstance (Fig. 4) can once again be attributed to a limited softening of the coating probably owing to frictional heat generation.

The values of the coefficient of friction obtained in this study range between 0.26 and 0.62 with an average of around 0.4. Visual examination of a zirconia ball reveals a clear spot formed by transfer of coating material after running the wear test for about 100 m or so. Undoubtedly, the coating material adheres to zirconia and perhaps to steel as well, during rubbing. Similar results have been reported by Dubois [7], De Palo et al. [23] and Fleury et al. [24,25]. It has been observed in these studies that two hard materials in contact lead to formation of small particles by fracture. These particles are picked up from the wear track by the harder member of the rubbing pair and gradually a layer of transferred material forms on it. The contact of dissimilar materials is thus transformed to a contact of similar materials and this results in high value of coefficient of friction. In this case, however, the friction experiments has been undertaken for a distance of 10 m only and the thickness of the transfer layer formed thereof is likely to be very small. The high friction coefficient observed in this study can thus be partly accounted for, by the presence of the thin layer of transferred material mentioned above. Also, it can be speculated that the other possible reason for such a value of the coefficient of friction is the presence of crystalline phases in the coating itself [20,26].

3.3. Coating wear

Fig. 15 is a record of the mass loss in wear with sliding distance. In the first 50 m of sliding the wear rate is low. During the contact between two hard surfaces, the zirconia ball undergoes fracture and the sharp edges of the fractured zirconia ball and the fractured zirconia particles cause abrasion on the coated surface. Also the metal from the coating is transferred to the zirconia ball and a contact between like materials (the metallic coating and the transferred layer of the coating on the zirconia surface) is established. The mechanism of wear from this point onwards

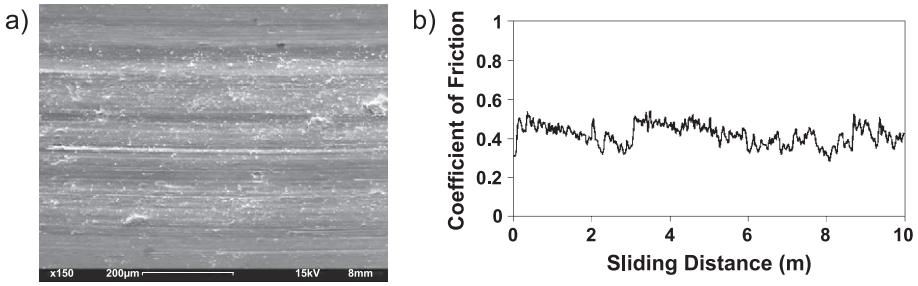

Fig. 10. (a) Higher magnification SE image of the wear tracks of Fig. 9 at normal load of 25 N for a velocity of 0.1 m/s and (b) the corresponding coefficients of friction.

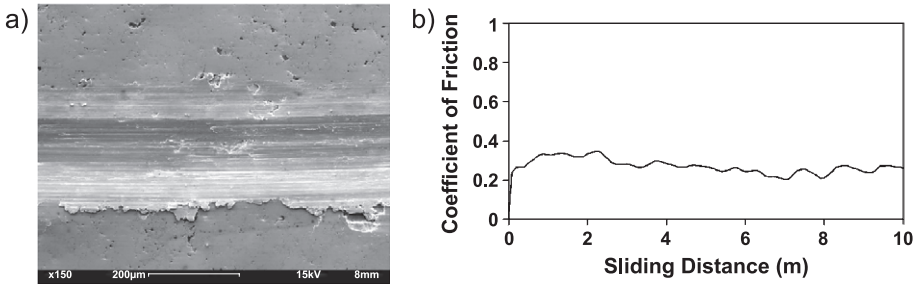

Fig. 11. (a) Higher magnification SE image of the wear tracks of Fig. 9 at normal load of 25 N for a velocity of 0.4 m/s and (b) the corresponding coefficients of friction.

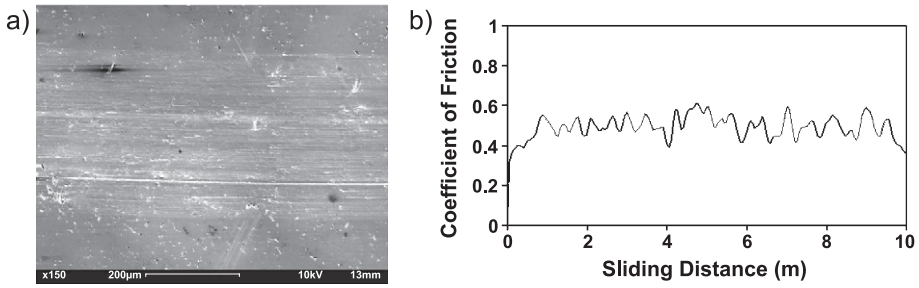

Fig. 12. (a) SE images of the wear track of a 10-mm diameter steel ball and normal load of 10 N. The sliding velocity is 0.5 m/s. (b) shows the corresponding coefficients of friction.

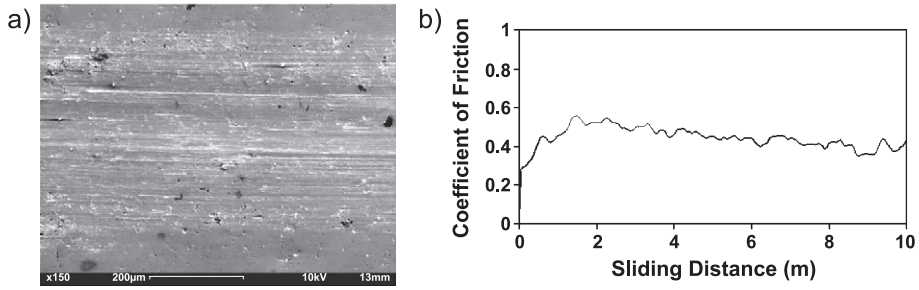

Fig. 13. (a) SE images of the wear track of a 10-mm diameter steel ball and normal load of 30 N. The sliding velocity is 0.5 m/s. (b) shows the corresponding coefficients of friction.

is adhesive. Beyond 100 m, the wear rate increases again and delamination comes into play. Fig. 16a and b illustrates this situation. Subsurface cracks grow during the tribo-action of the zirconia ball on the coating surface. This crack growth is encouraged by two factors; the high defect density of thermally sprayed coatings and the inherent brittleness of

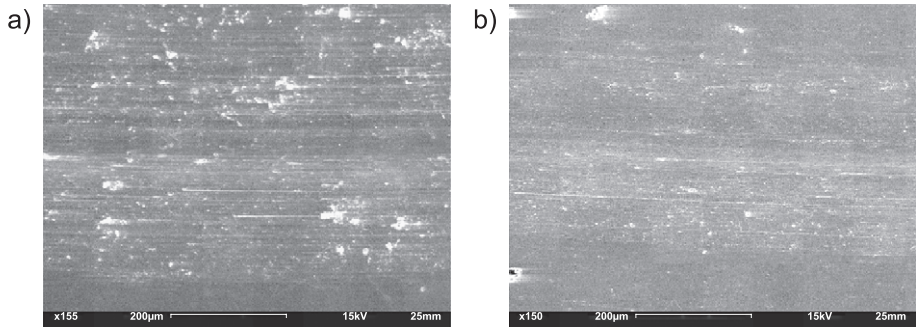

Fig. 14. (a) and (b) show the influence of sliding velocity of 0.1 and 0.8 m/s, respectively, on the wear track at a normal load of 30 N.

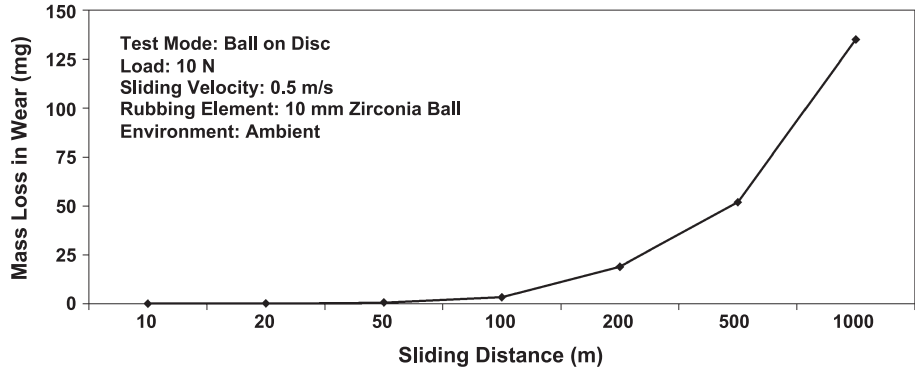

Fig. 15. Loss of mass in wear of the quasicrystal coating with sliding distance (in logarithmic scale) during rubbing against a zirconia ball.

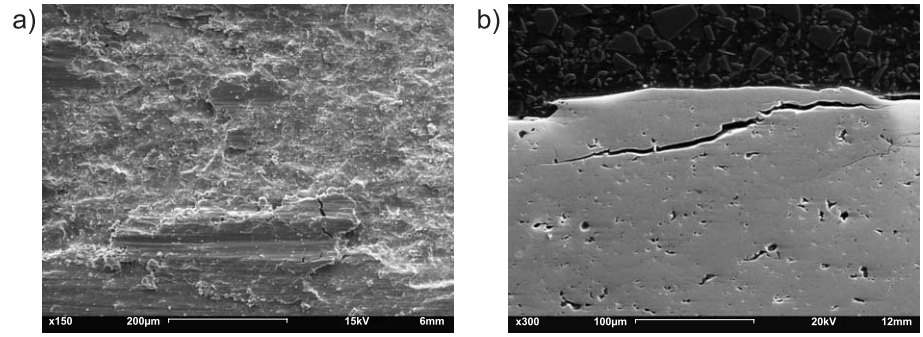

Fig. 16. The SE image (a) top view and (b) side view of a worn coating after rubbing against a zirconia ball over a sliding distance of 100 m with the parameters given in Fig. 15.

the quasicrystals. When the crack finally reaches the surface, a delaminated particle is dislodged from the coating. This explains a sudden growth of the wear rate of the coating.

4. Conclusions

1. At the low velocity regime, i.e., up to 0.2 m/s, motion of the zirconia rubbing element along the coated surface is of "stick-slip" nature. The plastic deformation involved is limited. The friction force shows periodic growth and decay. It is speculated that the temperature of the contact is low enough for the QC coating to retain its hardness. The zirconia rubbing element undergoes fracture owing to the contact with the hard QC coating. The friction between the sliding elements is high.
2. As the velocity is raised to 0.4 m/s and beyond, the rise in contact temperature apparently is high enough to soften the QC coating and makes it plastically deformable under the contact pressure. The low thermal conductivity of the QC helps in the retention of the high temperature and the resulting softness of the coating. No fractured zirconia particles are found. The softened QC layer provides a low friction path to sliding.
3. The friction and wear scenario at a low load, i.e., up to 10 N is somewhat similar to that in the low velocity regime. Plastic deformation of the coating is limited, fractured zirconia particles are abundant, mean coefficient of friction is high and the instantaneous coefficient of friction shows large variations. These, once again, can be attributed to the expected low contact temperature and the resulting high hardness of the coating undergoing rubbing against zirconia.
4. It is speculated that, as the normal load reaches 20 N, the contact temperature is high enough to bring about softening of the top layer of the coating, which in turn provides a low friction path.
5. During rubbing a thin layer of the coating material is transferred to the rubbing counterpart transforming the contact to a self-mated type of contact and this is likely to raise the value of the coefficient of friction for the pair of materials considered in this study.
6. When the zirconia ball is replaced with steel, no such abrupt transformation of wear mechanism occurs. This can be attributed to the higher thermal conductivity of steel, by dint of which it can transfer the heat generated at the contact. As a result, the coating retains its hardness to a large extent. The reduction in friction is also low. No fracture has been detected at any of the applied loads.
7. When sliding is continued to a longer distance against a zirconia ball, the wear mechanism is abrasive up to a sliding distance of 50 m. The abrasion is attributed to the sharp edges of the partially fractured zirconia ball and this wear mechanism accounts for a low wear rate. Beyond a sliding distance of 50 m, a layer of coating is transferred to the zirconia ball and the contact between like materials is established. The wear mechanism is adhesive and the corresponding wear rate also is higher. Beyond a sliding distance of 100 m, the wear rate is still higher and it is attributed to a delamination mode of wear.

Acknowledgements

The authors acknowledge the services rendered by Mr. H.-P. Feuz in relation to the tribological experiments. The authors are also thankful to the EMPA metallography team for the SEM and related work. In addition, the authors would like to express their thankfulness to Dr. A. Kulkarni, State University of New York at Stony Brook, and Dr. N. Margadant, EMPA for their kind help in getting the thermal diffusivity measurements done.

References

[1] D. Shechtman, I. Blech, D. Gratias, J.W. Cahn, Phys. Rev. Lett. 53 (20) (1984) 1951.
[2] Y. Massiani, S. Ait Yaazza, J.P. Crousier, J.M. Dubois, J. Non-Cryst. Solids 159 (1–2) (1993) 92.
[3] T. Klein, O.G. Symko, Appl. Phys. Lett. 64 (4) (1994) 431.
[4] J.M. Dubois, S.S. Kang, S. Von Stebut, J. Mater. Sci. Lett. 10 (9) (1991) 537.

[5] C.J. Jenks, P.A. Theil, MRS Bull. 22 (11) (1997) 55.
[6] F. Cyrot-Lackmann, Mater. Sci. Eng., A 294–296 (2000) 611.
[7] J.-M. Dubois, Mater. Sci. Eng., A 294–296 (2000) 4.
[8] D.J. Sordelet, S.D. Widener, Y. Tang, M.F. Besser, Mater. Sci. Eng., A 294–296 (2000) 834.
[9] J.M. Dubois, S.S. Kang, A. Perrot, Mater. Sci. Eng., A 179–180 (1994) 122.
[10] D.J. Sordelet, M.F. Besser, I.E. Anderson, J. Therm. Spray Technol. 5 (2) (1996) 161.
[11] J.P. Davis, E.H. Majzoub, J.M. Simmons, K.F. Kelton, Mater. Sci. Eng., A 294–296 (2000) 104.
[12] P.A. Thiel, A.I. Goldman, C.J. Jenks, in: Z.M. Stadnik (Ed.), Physical Properties of Quasicrystals, Springer Series in Solid State Science, vol. 126, Springer-Verlag, Berlin, Germany, 1999, p. 327.
[13] K.F. Kelton, W.J. Kim, R.M. Stroud, Appl. Phys. Lett. 70 (20) (1997) 3230.
[14] F.J. Hermanek, in: C.C. Berndt (Ed.), Proc. 1st International Thermal Spray Conference—Thermal Spray: Surface Engineering via Applied Research, ASM International, Materials Park, OH, 2000, p. 567.
[15] E. Lugscheider, C. Herbst-Dederichs, A. Reimann, in: C.C. Berndt (Ed.), Proc. 1st International Thermal Spray Conference—Thermal Spray: Surface Engineering via Applied Research, ASM International, Materials Park, OH, 2000, p. 843.
[16] A. Reimann, E. Lugscheider, in: C.C. Berndt, K.A. Khor, E. Lugscheider (Eds.), Conf. Proc. of Thermal Spray 2001—New Surfaces for a New Millennium, ASM International, Materials Park, OH 44073-0002, 2001, p. 33.
[17] D.J. Sordelet, P.D. Krotz, R.L. Daniel Jr., M.F. Smith, in: C.C. Berndt, S. Sampath (Eds.), Proc. 8th National Thermal Spray Conference—Advances in Thermal Spray Science and Technology, ASM International, Materials Park, OH, 1995, p. 627.
[18] J.E. Shield, A.I. Goldman, I.E. Anderson, T.W. Ellis, R.W. McCallum, D.J. Sordellet, US Patent # 5,433,978.
[19] D.J. Sordelet, M.F. Besser, J.L. Logsdon, Mater. Sci. Eng., A 255 (1998) 54.
[20] P.P. Bandyopadhyay, P. Kern, S. Siegmann, J. Mater. Sci. 39 (2004) 6101.
[21] E.H. Majzoub, Ph.D. thesis, Ti Based Icosahedral Quasicrystals and Approximants: Phase Formation, Cluster Structure and Hydrogenation, Washington University, 2000.
[22] J. Pezdirnik, J. Vizintin, B. Podgornik, Tribol. Int. 32 (1999) 481.
[23] S. De Palo, S. Usmani, S. Sampath, D.J. Sordelet, M.F. Besser, in: C.C. Berndt (Ed.), Proceedings of United Thermal Spray Conference—Thermal Spray: A United Forum for Scientific and Technological Advances, ASM International, Materials Park, OH, 1997, p. 135.
[24] E. Fleury, Y.C. Kim, J.S. Kim, D.H. Kim, W.T. Kim, H.S. Ahn, S.M. Lee, J. Alloys Compd. 342 (2002) 321.
[25] E. Fleury, Y.C. Kim, J.S. Kim, H.S. Ahn, S.M. Lee, W.T. Kim, D.H. Kim, J. Mater. Res. 17 (2) (2002) 492.
[26] L.M. Zhang, P. Brunet, Z.C. Zhang, C. Dong, J.M. Dubois, Tribol. Lett. 8 (2000) 233.